IEEE Access
Multidisciplinary | Rapid Review | Open Access Journal

Received June 22, 2020, accepted July 1, 2020, date of publication July 7, 2020, date of current version July 20, 2020.

Digital Object Identifier 10.1109/ACCESS.2020.3007784

Higher-Order Super-Twisting Control for Trajectory Tracking Control of Skid-Steered Mobile Robot

IMAD MATRAJI[1], (Member, IEEE), KHALED AL-WAHEDI[2], (Member, IEEE), AND AHMED AL-DURRA[2], (Senior Member, IEEE)

[1]Great Wall Motor Company Limited, Baoding 071000, China
[2]Electrical Engineering and Computer Science Department, Khalifa University, Abu Dhabi, United Arab Emirates

Corresponding author: Imad Matraji (matraji.imad@gmail.com)

ABSTRACT In this paper, Higher-Order Super-Twisting control (HOST) is designed and implemented for trajectory tracking control of four wheels Skid-Steered Mobile Robot (SSMR). The conventional Super-Twisting (ST) Second-Order Sliding Mode Control (SOSMC) is robust, yet it has two main drawbacks for such a system, 1) the chattering phenomena persists on the system inputs and outputs which leads to vibration in the robot motors and 2) the SSMR system has a relative degree equal to two. Therefore, the ST control design requires a sliding variable containing error derivatives, which only permit asymptotic convergence. For that, a higher-order controller is required for this control structure, which is designed for second order sliding variable, in order to obtain a robust controller with finite-time convergence. The HOST control can reduce chattering in steady-state compared with conventional ST-SOSMC and converge the state variables in finite time. The performance of this controller has been validated experimentally on Pioneer P3AT SSMR robot. The experimental results show good performance under parametric uncertainty variations and external disturbance with neglected chattering.

INDEX TERMS Trajectory tracking control, higher order sliding mode, super twisting algorithm, skid-steered mobile robot.

I. INTRODUCTION

Autonomous mobile robots are used in several applications mainly where human intervention or guidance is not possible. The Skid Steered Mobile Robot (SSMR) vehicle moves by creating differential torques through wheel motors on opposite sides. These robots are known for their mechanical robustness as they do not need a steering system and can simply move on a rough surface. Their trajectory tracking control is very difficult, as they tend to skid laterally on curved paths. The mathematical model of the robot is divided into two parts kinematic model and dynamic model [1]. In contemporary literature, most controller designs take into account only the kinematics of SSMR robots. In practice, however, trajectory tracking requires robot dynamics to be taken into account in the control design for robustness purposes [2].

In the literature, many papers address the trajectory tracking control of SSMR. In [3], a robust controller is presented which uses exponential stabilizing state feedback and it also generates friction estimations. This controller has been shown to work for straight paths only, through simulation. A modified Proportional-Integral-Derivative (PID) controller has been developed in [4]. In [5], [6], the authors address a method for finding controller gains according to actuator saturation limits. This method is prone to steady state errors, and it leaks for robustness against uncertainties. In [7], an adaptive PID approach has been used, dependent upon initial estimations, which may not be precise. This controller has been shown good performance only on short trajectories. Other approaches include fuzzy logic and model predictive controllers are presented in [8], [9]; all of them suffer similar drawback, which is the requirement of full knowledge of the system behavior. In [10], the authors proposed a feedback hierarchical controller for velocity tracking using a modular observer to estimate the vehicle longitudinal velocity and input-to-state stability theory. In [11], Adaptive Neural Network based trajectory tracking control for SSMR is proposed. Fuzzy logic controller has been implemented in [12]. Despite

The associate editor coordinating the review of this manuscript and approving it for publication was Haibin Sun.

the good performance of the proposed controller in terms of precision and speed response, the fuzzy logic controller depends on the number of rules integrated into the control design.

In [13], [14], a first order Sliding Mode Control (SMC) is applied for trajectory tracking control. This controller has good performance and no steady state error. SMC suffers from high frequency oscillations in the system outputs. This oscillation is the classical sliding mode drawback, and it is known by chattering. The authors in [15]–[17] and [16]–[18] used a Second-Order SMC (SOSMC) based on the Super-Twisting algorithm (ST) and the proposed controller designs showed good performance. In [19], [20], SOSMC has been designed and experimentally implemented for quadrotor trajectory tracking. SOSMC algorithms reduce chattering while maintaining the steady state performance level. But as the SSMR has a relative degree 2 with the respect to sliding variables, therefore the sliding variables were designed using derivative of the controller error in order to decrease the relative degree of the system. The state variables converge asymptotically to their steady states [21]. In case the system uncertainty bounds are known, then robust controller gains can be maximized in order to improve the controller performance in terms of response time, which results in chattering. For these reasons, Higher-Order Sliding Mode Control (HOSMC) was developed in order to design a controller for higher-order sliding variable by maintaining the same features of a classical SMC [22]–[24]. The authors in [25] proposed an adaptive SOSMC in which the gains adapt dynamically to the system parametric variations. The controller gains increase during transit state and decrease when a predefined neighborhood of the sliding variable is achieved. This algorithm is a good solution when the system suffers from unknown parametric variations, and it reduces the chattering at steady state.

In this work, the control design problem using Higher-Order Super-Twisting (HOST) controller based on higher-order sliding mode control is addressed [26]. HOST controller is developed for perturbed chain of integrators for arbitrary order. The controller ensures finite time convergence of the sliding variable and its r^{th} derivatives to zero, by using a continuous control signal through the explicit construction of strict homogeneous Lyapunov function. The principal contributions are; First, the concept of higher-order sliding variable is introduced in order to ensure a finite time convergence of double chain of integrators. The higher-order sliding mode controller is designed for controlling SSMR system which has a relative degree equal to two with respect to the sliding variable; Second, the chattering can be reduced which improves the control performance. Hence, it provides smooth operation of the robot motors without any vibration due to its higher order controller design. This controller maintains the features of the conventional sliding mode controller, such as robustness under parametric uncertainty and external disturbance. The proposed control design has been validated experimentally using the Pioneer P3AT SSMR robot. The dynamic model used in this work is based on [3], [7]. Experiments were conducted for comparing the proposed control design performance with other algorithms in practice. Furthermore, image processing has been applied to verify the trajectory tracking of different algorithms.

The rest of the paper is structured as follows: the mathematical model of the system is presented in Section II. In Section III, the Higher-Order Super-Twisting mode controller is described. In Section IV, the proposed control design is discussed. Experimental validation and comparison studies are included in Section V. While Section VI contains concluding remarks.

II. PROBLEM FORMULATION

The SSMR model is based on [7], which is subsequent to [3]. The main assumptions are:

- Robot speed below 10 km/h;
- Perfect longitudinal traction (no wheel slip);
- Rigid body movement restricted to 2D plane;
- Lateral effort on tires proportional to the vertical load.

The state vector is given by $q = [x\ y\ \theta]^T$, where x and y provide the vehicle center in the earth frame, and θ provides orientation in the 2D frame. The state dynamics q are

$$\dot{q} = \begin{bmatrix} \cos\theta & -d\sin\theta \\ \sin\theta & d\cos\theta \\ 0 & 1 \end{bmatrix} \begin{bmatrix} v \\ \omega \end{bmatrix}, \tag{1}$$

where v and ω are the linear and angular velocities, and d is the distance between the robot's center of rotation and center of gravity. The dynamic model is represented by the linear and angular acceleration and given by the state vector $\eta = [v\ \omega]^T$. The model can be written as follows:

$$\dot{\eta} = \begin{bmatrix} \frac{c_3}{c_1}\omega^2 - \frac{c_4}{c_1}v \\ -\frac{c_5}{c_2}v\omega - \frac{c_6}{c_2}\omega \end{bmatrix} + \begin{bmatrix} \frac{1}{c_1} & 0 \\ 0 & \frac{1}{c_2} \end{bmatrix} \begin{bmatrix} v_r \\ \omega_r \end{bmatrix}, \tag{2}$$

where, v_r and ω_r are the system's control inputs, and they are reference linear velocity and reference angular velocity respectively. q and η are measured. With $c_1, \ldots, c_6$ are positive constants that represent the robot's physical parameters, and they are given as follows:

$$\begin{aligned} c_1 &= \left[\frac{R}{k_a}(mk_r^2 + 2I_e) + 2k_r k_{dt}\right]\frac{1}{2k_r k_{pt}}, \\ c_2 &= \left[\frac{R}{k_a}(I_e k_d^2 + 2k_r^2(I_z + mb^2)) + 2k_r k_d k_{dr}\right] \\ &\quad \frac{1}{2k_r k_d k_{pr}}, \\ c_3 &= \frac{R}{k_a}\frac{mbk_r}{2k_{pt}}, \quad c_5 = \frac{R}{k_a}\frac{mbk_r}{k_d k_{pr}}, \\ c_4 &= \frac{R}{k_a}\left(\frac{k_a k_b}{R} + B_e\right)\frac{1}{k_r k_{pt}} + 1, \\ c_6 &= \frac{R}{k_a}\left(\frac{k_a k_b}{R} + B_e\right)\frac{k_d}{2k_r k_{pr}} + 1, \end{aligned} \tag{3}$$

with, m is the robot mass, I_z is the moment of inertia, R is the electrical resistance of motors, k_b is the electromotive constant of motors, k_a is the constant of torque motors, B_e is the coefficient of friction, I_e is the moment of inertia of each group rotor-reduction gear-wheel, k_r is the radius of the wheels, b is the distance from the wheel to the gravity, k_d is the width of the robot. It is assumed that the robot servos have proportional derivative controllers to control the rotation speed of each motor, with proportional gains $k_{pt} > 0$ and $k_{pr} > 0$, and derivative gains $k_{dt} > 0$ and $k_{dr} > 0$.

It is hard to estimate the exact values of the system parameters as they depend on the robot's construction and specs as well as the in-built velocity control loops. Each parameter consists of two parts; estimated nominal value and uncertain value [27]:

$$\begin{aligned} c_1 &= c_{01} + \delta c_1, \quad c_2 = c_{02} + \delta c_2, \\ c_3 &= c_{03} + \delta c_3, \quad c_4 = c_{04} + \delta c_4, \\ c_5 &= c_{05} + \delta c_5, \quad c_6 = c_{06} + \delta c_6, \end{aligned} \tag{4}$$

where c_{0i} is the nominal value of parameter i, and δc_i represents uncertainty in its knowledge, i.e. $|\delta c_i| \leq \delta c_{0i} < |c_{0i}|$, where δc_{0i} is a known positive bound. The expected variation in the parameters of our system is estimated to be $\pm 20\%$ of their nominal values.

A. CONTROL OBJECTIVE

The control objective for our robot is to track a given trajectory:

$$q_r = [x_r,\ y_r]^T. \tag{5}$$

where x_r and y_r are reference positions defined in the earth frame. q_r is generated using a virtual kinematic model such that it is C^2 continuous with its Lipschitz constant dependent upon the upper limit constraints on the robot's velocities and accelerations.

III. HIGHER-ORDER SLIDING MODE CONTROL

During the operation on terrain, a robot has to deal with uncertain external conditions throughout. SMC is a simple solution, which reacts immediately against system deviations in presence of parametric variations as well as external disturbance. However, this method has the drawback of "chattering", i.e. high frequency oscillations in the system output. Chattering can be avoided by acting on the higher-order time derivatives of the system [28]. The HOST algorithm based on HOSMC, proposed recently in [26], is adopted for this application. This algorithm is a higher-order version of the very well known conventional ST algorithm proposed in [29]. In section III-A, the major points of the design and proof of HOST is presented. The interested reader can refer to the original papers [26], [30] for more detailed discussion about HOST. In section III-B, robust exact differentiator is presented which is used to estimate the first time derivative of the sliding variables.

A. HIGHER-ORDER SUPER-TWISTING ALGORITHM

Let us consider the following nonlinear system of relative degree r:

$$\begin{aligned} \dot{x} &= f(x) + g(x)u, \\ y &= s(x), \end{aligned} \tag{6}$$

where $x \in \mathbb{R}^n$ is the state vector whose dynamics depend upon the smooth functions f and g. The control input is $u \in \mathbb{R}$ and $s(x)$ represents the output function, which is also the sliding variable. The control objective is to force this variable and their $r-1$ derivatives to zero. The r derivative of $s(x)$ is:

$$s^r = \varphi(t) + \gamma(t)u(t). \tag{7}$$

The functions $\varphi(t)$ and $\gamma(t)$ are assumed to be bounded, i.e. $\forall u \in \mathcal{U}$ and $\forall x \in \mathcal{X}$,

$$\exists\ \bar{\varphi} > 0,\ \bar{\gamma} > 0,\ \textit{and}\ 0 < \gamma_m \leq \gamma(t) \leq \gamma_M,\ |\dot{\varphi}(t)| \leq \varphi. \tag{8}$$

The HOST algorithm is defined by the following control law

$$u = k_P v_0 - k_I \int \partial_r V_1 dt, \tag{9}$$

where k_I and k_P are positive constants with $k_P > 1$. $\partial_r V_1$ is the partial derivative of V_1 with respect to the $r-th$ coordinate s^{r-1} and V is continuous positive function $\mathbb{R}^r \to \mathbb{R}_+$. v_0 is a feedback law and finite time stable.

In [26], two candidates for v_0 have been proposed; Hong's controller and modified Hong's controller. In this paper, the Hong's Controller is adopted as it is continuous, contrary to the modified Hong's controller, which suffers of some discontinuity before convergence. Hence, the feedback controller v_0 and Lyapunov function V_1 are determined using a hybrid form between the continuous controller proposed by [30] and the terminal sliding mode approach proposed by [31]. This controller is constructed by induction method starting by $l_1, l_2, \ldots, l_r$. At each iteration "i", the controller u_i stabilizes the "i" chain of integrators. The feedback controller v_0 is equal to the continuous function u_r which is given as a function of u_i with $i = 0, \ldots, r-1$ and it is given as follow

$$\begin{aligned} u_0 &= 0, \\ u_1 &= -l_1 \left\lfloor \lfloor s \rceil^{\beta_0} - \lfloor u_0 \rceil^{\beta_0} \right\rceil^{\frac{p_1}{p_0 \beta_0}}, \\ &\vdots \\ u_i &= -l_i \left\lfloor \left\lfloor s^{i-1} \right\rceil^{\beta_{i-1}} - \lfloor u_{i-1} \rceil^{\beta_{i-1}} \right\rceil^{\frac{p_i}{p_{i-1}\beta_{i-1}}}, \\ v_0 &= -l_r \left\lfloor \left\lfloor s^{r-1} \right\rceil^{\beta_{r-1}} - \lfloor u_{r-1} \rceil^{\beta_{r-1}} \right\rceil^{\frac{p_r}{p_{r-1}\beta_{r-1}}}, \end{aligned} \tag{10}$$

where $l_i > 0, p_i = 1 + (i-1)\kappa, \kappa = -1/(r+1) < 0, \beta_0 = p_2$ and $\beta_i = (\beta_0 + 1)/p_{i+1} - 1$, and with

$$\lfloor x \rceil^{\alpha} = |x|^{\alpha}\, sign(x). \tag{11}$$

The Lyapunov function V_1 is given since v_0 and V_1 are constructed simultaneously. Consider the Lyapunov function

V_0 which proves the stability of the controller v_0

$$V_0 = \sum_{i=1}^{r} W_i, \tag{12}$$

where W_i is positive real-valued function and it is given by

$$W_i = \frac{1}{\beta_{i-1}+1}\left(|s^{i-1}|^{\beta_{i-1}+1} + \beta_{i-1}|u_{i-1}|^{\beta_{i-1}+1}\right) - s^{i-1}\lfloor u_{i-1}\rceil^{\beta_{i-1}}, \tag{13}$$

Then, there exist $l_1, l_2, \ldots, l_r > 0$ such that the time derivative of V_0 satisfies $\dot{V}_0 \leq -lV_0^{((2+2\kappa)/(2+\kappa))}$, where $l > 0$.
The Lyapunov function V_1 is given as function of V_0 which also proves the stability of "r" chain of integrators. V_1 is given as

$$V_1 = V_0^{\lambda}/\lambda, \tag{14}$$

with $\lambda := 2/(2r-1)$. Note that, $1-\lambda = \frac{\beta_{r-1}}{\beta_{r-1}+1}$. Then, the partial derivative of V_1 with respect to the $r-th$ coordinate s^{r-1} given in Eq.(9) can be written as follow

$$\partial_r V_1 = \frac{\lfloor s^{r-1}\rceil^{\beta_{r-1}} - \lfloor u_{r-1}\rceil^{\beta_{r-1}}}{V_0^{\frac{1}{\beta_{r-1}+1}}}. \tag{15}$$

The global Lyapunov function W is constructed to be a positive definite proper Lyapunov function. It's homogenous and a strong Lyapunov function, and it is given as

$$W = (V_1 + \xi^2/2)^{(3/2)} - As^{(r-1)}\xi, \tag{16}$$

with

$$\xi(t) = -k_I \int_0^t \partial_r V_1 d\tau + \phi(t)/\gamma(t), \tag{17}$$

where $\xi(0) = 0$, and A is positive and small enough. Then, the time derivative of the global Lyapunov function, $\dot{W} \leq -mW^{2/3}$ where $m > 0$. This proves that the controller u, given in Eq.(9), stabilizes Eq.(7) to the origin in finite-time.

B. EXACT DIFFERENTIATOR

In order to estimate the derivative of the reference trajectory, let us introduce the real time robust exact differentiator [32]

$$\begin{aligned} z_0 &= -\epsilon_2\sqrt{L}\sqrt{|z_0-\rho|}sign(z_0-\rho) + z_1, \\ z_1 &= -\epsilon_1 Lsign(z_1 - z_0), \end{aligned}$$

where z_0 and z_1 are the real time estimates of ρ and $\dot{\rho}$, respectively. The differentiator is parametrized as $\epsilon_1 = 1.1$, $\epsilon_= 1.5$, which leaves L is to be tuned according to $|\ddot{\rho}| \leq \rho$.

IV. CONTROL DESIGN FOR SSMR

For Multi-Input Multi-Output (MIMO) systems, HOSMC requires two sliding variables. The sliding variables for the SSMR, s_1 and s_2, are:

$$\begin{aligned} s_1 &= x - x_r, \\ s_2 &= y - y_r \end{aligned} \tag{18}$$

where x_r and y_r are the position x and y of the reference trajectory respectively.

The control structure can be seen in Fig.1.

Consider the first time derivative $\dot{s}_1$ and $\dot{s}_2$ of s_1 and s_2, respectively.

$$\begin{aligned} \dot{s}_1 &= v\cos\theta - d\omega\sin\theta - \dot{x}_r, \\ \dot{s}_2 &= v\sin\theta + d\omega\cos\theta - \dot{y}_r. \end{aligned} \tag{19}$$

It can be seen that the system control inputs $[v_r,\ \omega_r]^T$ do not appear in the first time derivative of the sliding variables. Therefore, the second time derivative $\ddot{s}_1$ and $\ddot{s}_2$ of s_1 and s_2 is considered, and they are given as follows:

$$\begin{aligned} \ddot{s}_1 &= \left(\frac{c_3}{c_1}\omega^2 - \frac{c_4}{c_1}v + \frac{v_r}{c_1}\right)\cos\theta - v\omega\sin\theta \\ &\quad - d\left(-\frac{c_5}{c_2}v\omega - \frac{c_6}{c_2}\omega + \frac{\omega_r}{c_2}\right)\sin\theta \\ &\quad - d\omega^2\cos\theta - \ddot{x}_r, \\ \ddot{s}_2 &= \left(\frac{c_3}{c_1}\omega^2 - \frac{c_4}{c_1}v + \frac{v_r}{c_1}\right)\sin\theta + v\omega\cos\theta \\ &\quad + d\left(-\frac{c_5}{c_2}v\omega - \frac{c_6}{c_2}\omega + \frac{\omega_r}{c_2}\right)\cos\theta \\ &\quad - d\omega^2\sin\theta - \ddot{y}_r, \end{aligned} \tag{20}$$

The system control inputs $[v_r,\ \omega_r]^T$ appear in the second derivative of the sliding variable then the relative degree of the SSMR with respect to the sliding variables is equal to two. The second time derivative of s_1 and s_2 can be simplified;

$$\begin{aligned} \ddot{s}_1 &= \phi_1 + \gamma_1 v_r, \\ \ddot{s}_2 &= \phi_2 + \gamma_2 \omega_r, \end{aligned} \tag{21}$$

with

$$\begin{aligned} \phi_1 &= \phi_{01} + \delta\phi_1, \quad \gamma_1 = \gamma_{01} + \delta\gamma_1, \\ \phi_2 &= \phi_{02} + \delta\phi_2, \quad \gamma_2 = \gamma_{02} + \delta\gamma_2, \end{aligned} \tag{22}$$

where ϕ_{01}, ϕ_{02}, γ_{01} and γ_{02} are based on the nominal parameters c_{0i} and $\delta\phi_1$, $\delta\phi_2$, $\delta\gamma_1$ and $\delta\gamma_2$ are fund by varying parameters to $+-20\%$ and they are based on the uncertain parameters δc_{0i}. The explicit form of functions ϕ_1, ϕ_2, γ_1 and γ_2 are given in Appendix A.

In order to keep the controller gains low and decouple the controllers, a FeedBack Linearization (FBL) is used for simplifying the system by pre-compensation of the known nonlinear part

$$\begin{aligned} v_r &= \gamma_{01}^{-1}[v_1 - \phi_{01}], \\ \omega_r &= \gamma_{02}^{-1}[v_2 - \phi_{02}], \end{aligned} \tag{23}$$

where v_1 and v_2, control double chain of integrators,

$$\begin{aligned} \ddot{s}_1 &= v_1 + \delta\phi_1 + \delta\gamma_1 v_r, \\ \ddot{s}_2 &= v_2 + \delta\phi_2 + \delta\gamma_2 \omega_r, \end{aligned} \tag{24}$$

by applying HOST control law given in Eq.(9), the controllers v_1 and v_2 are given by

$$v_1 = k_{1,P}v_{1,0} - \int k_{1,I}\partial_2 V_{1,1} dt,$$

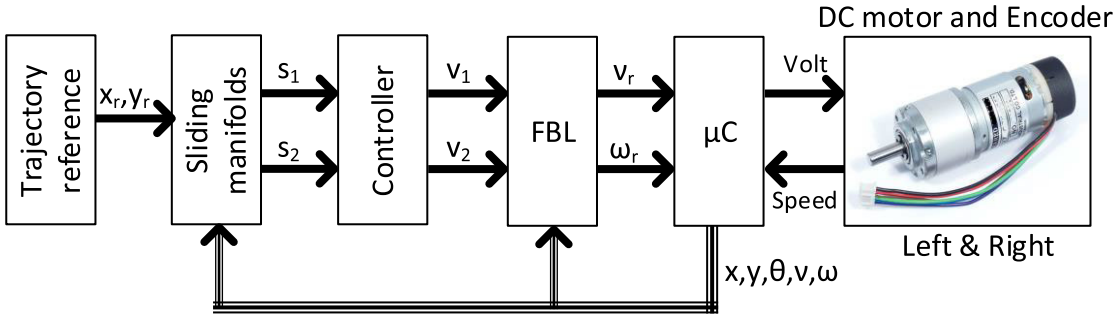

FIGURE 1. Proposed control structure.

$$v_2 = k_{2,P} v_{2,0} - \int k_{2,I}\, \partial_2 V_{2,1} d. \tag{25}$$

Applied Eq.(23) to Eq.(21), the sliding manifolds can be written as follows

$$\begin{aligned} \ddot{s}_1 &= \hat{\phi}_1 + \hat{\gamma}_1 \left(k_{1,P} v_{1,0} - \int k_{1,I}\, \partial_2 V_{1,1} dt \right), \\ \ddot{s}_2 &= \hat{\phi}_2 + \hat{\gamma}_2 \left(k_{2,P} v_{2,0} - \int k_{2,I}\, \partial_2 V_{2,1} dt \right). \end{aligned} \tag{26}$$

with

$$\begin{aligned} \hat{\phi}_1 &= \delta\phi_1 - \phi_{01} \frac{\delta\gamma_1}{\gamma_{01}}, \\ \hat{\phi}_2 &= \delta\phi_2 - \phi_{02} \frac{\delta\gamma_2}{\gamma_{02}}, \\ \hat{\gamma}_1 &= 1 + \frac{\delta\gamma_1}{\gamma_{01}}, \\ \hat{\gamma}_2 &= 1 + \frac{\delta\gamma_2}{\gamma_{02}}, \end{aligned} \tag{27}$$

where $\hat{\phi}_1$, $\hat{\phi}_2$, $\hat{\gamma}_1$ and $\hat{\gamma}_2$ follow the same conditions given in Eq.(8). The controller parameters are set as follows $k_{1,P} = k_{2,P} = 0.5$ and $k_{1,I} = k_{2,I} = 0.01$.

To avoid the redundancy in the controller equations, the functions used for the controller v_1 and v_2 are denoted by $j = 1, 2$ respectively. $v_{j,0}$ and $\partial_2 V_{j,1}$ are calculated as presented in Eq.(10) and Eq.(15) for the second order. They are given as

$$\begin{aligned} v_{j,0} &= u_{j,2}, \\ \partial_2 V_{j,1} &= \frac{\lfloor \dot{s}_j \rceil^{\beta_{j,1}} - \lfloor u_{j,1} \rceil^{\beta_{j,1}}}{V_{j,0}^{\frac{1}{\beta_{j,1}+1}}}, \end{aligned} \tag{28}$$

where

$$\begin{aligned} u_{j,0} &= 0, \\ u_{j,1} &= -l_{j,1} \left\lfloor \lfloor s_j \rceil^{\beta_{j,0}} - \lfloor u_{j,0} \rceil^{\beta_{j,0}} \right\rceil^{\frac{p_{j,1}}{p_{j,0}\beta_{j,0}}}, \\ u_{j,2} &= -l_{j,2} \left\lfloor \lfloor \dot{s}_j \rceil^{\beta_{j,1}} - \lfloor u_{j,1} \rceil^{\beta_{j,1}} \right\rceil^{\frac{p_{j,2}}{p_{j,1}\beta_{j,1}}}, \\ W_{j,1} &= \frac{1}{\beta_{j,0}+1} \left(|s_j|^{\beta_{j,0}+1} + \beta_{j,0} |u_{j,1}|^{\beta_{j,0}+1} \right) \\ &\quad - s_j \lfloor u_{j,0} \rceil^{\beta_{j,0}}, \\ W_{j,2} &= \frac{1}{\beta_{j,1}+1} \left(|\dot{s}_j|^{\beta_{j,1}+1} + \beta_{j,1} |u_{j,2}|^{\beta_{j,1}+1} \right) \\ &\quad - \dot{s}_j \lfloor u_{j,1} \rceil^{\beta_{j,1}}, \\ V_{j,0} &= W_{j,1} + W_{j,2}, \end{aligned} \tag{29}$$

with $l_{j,1} = 0.8$, $l_{j,2} = 1.5$, $\beta_{j,0} = 0.5$and $\beta_{j,1} = 4$,

V. EXPERIMENTAL IMPLEMENTATION AND RESULTS

A. EXPERIMENTAL SETUP

The experimental mobile robot setup consists of Pioneer 3AT mobile robot (Fig.2). This robot has a differential drive, fed by DC motors. A high-resolution quadrature encoder provides feedback to the primary microcontroller, which contains the PID velocity controller. The linear velocity, rotational velocity, linear acceleration and rotational acceleration are constrained to 0.7 m/s, 360 deg/s, and 0.2 m/s^2, 360 deg/s^2 respectively. An additional onboard PC is used to run higher level control algorithms, communicating with the primary microcontroller through a serial port at 5ms. The higher level control is run on MATLAB with sampling time set to half the communication rate, i.e. 10ms, to ensure good communication with the microcontroller. The system parameters $c_1, \ldots, c_6$ are given as follows:

$$\begin{aligned} c_1 &= 0.27, \quad c_2 = 0.25, \\ c_3 &= -0.0005, \quad c_4 = 1, \\ c_5 &= 0.003, \quad c_6 = 1.1. \end{aligned} \tag{30}$$

B. EXPERIMENTAL RESULTS

The reference trajectory is chosen as a circular path parameterized as a function of time:

$$\begin{aligned} x_r &= \cos(0.25t), \\ y_r &= \sin(0.25t). \end{aligned}$$

Experiments have been performed for different scenarios in order to validate and compare the performance of the proposed control design. Three complete circular cycles of the trajectory, amounting to 75s in total, have been applied. The first cycle is executed under nominal conditions where no additional uncertainties have been considered, the second

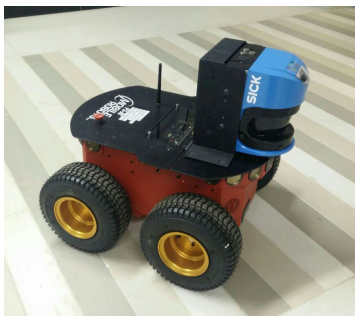

FIGURE 2. Pioneer 3AT SSMR.

cycle includes parametric uncertainty variations, and the third cycle employs a sudden shift in the trajectory reference center while returning the parameters to nominal:

$$x_r = \cos(0.25t) - 0.2,$$
$$y_r = \sin(0.25t) - 0.2.$$

All distances are given in meters. The robot is initialized on $(x = 0.2, y = 0, \theta = 0)$ in the earth frame. The performance of the presented HOST controller has been presented in relation with the conventional ST and PID algorithms.

1) COMPARISON BETWEEN ST AND PID ALGORITHMS

Let us first see how a conventional ST algorithm performs in comparison to PID controller. The PID controller is designed in order to control x and y to follow x_r and y_r, respectively. The errors are given as follow:

$$e_1 = x - x_r,$$
$$e_2 = y - y_r. \tag{31}$$

The ST sliding variables have a relative degree one and they are given as follow:

$$s_1 = \lambda_1 e_1 + \dot{e}_1,$$
$$s_2 = \lambda_2 e_2 + \dot{e}_2, \tag{32}$$

with λ_1 and λ_2 are positive constants.

The error responses are shown in Fig.3 and Fig.4. It can be seen that ST has faster response time against the PID, with similar steady state performance during the first cycle. The PID fails in the second cycle with hunting effect predominant. ST also outperforms the PID in response time during the step change of the third cycle. These results are further confirmed in the x and y position plot shown in Fig.5 and Fig.6. Fig.7 shows the trajectory in the x-y frame for both ST and PID controllers. Fig.8 and Fig.9 show the comparison of the control inputs v_r and ω_r, respectively. In the ST results, however, chattering is very clear, which is also obvious physically as the robot vibrates during experiments.

2) COMPARISON BETWEEN HOST AND ST ALGORITHMS

The comparison of HOST and ST algorithms is presented in this section. The error responses e_1 and e_2 are shown in Fig.10 and Fig.11, respectively. Noted that, the error responses and the sliding variables of the HOST are identical. During the first and third cycles, the HOST has a similar convergence

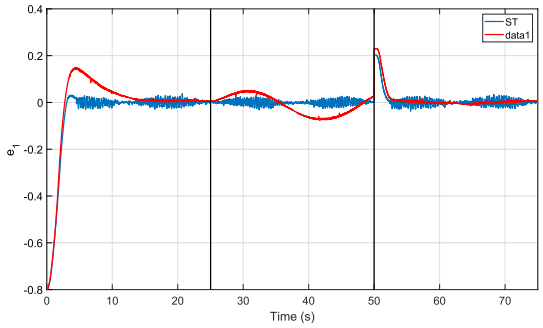

FIGURE 3. Error response e_1, comparison between Super-Twisting and Proportional Integral Derivative.

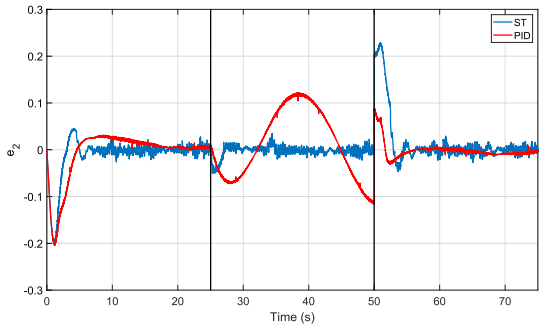

FIGURE 4. Error response e_2, comparison between Super-Twisting and Proportional Integral Derivative.

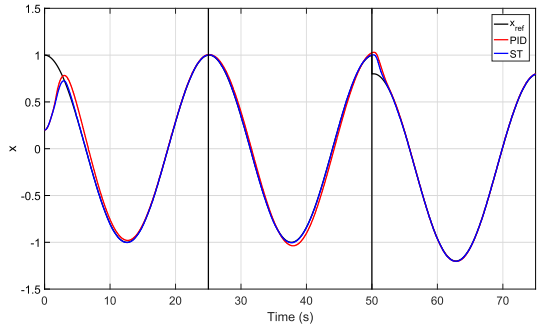

FIGURE 5. Position x response, comparison between Super-Twisting and Proportional Integral Derivative.

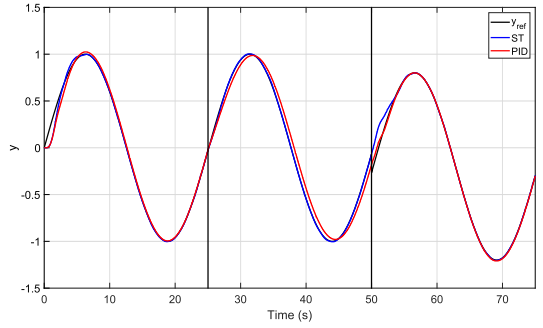

FIGURE 6. Position y response, comparison between Super-Twisting and Proportional Integral Derivative.

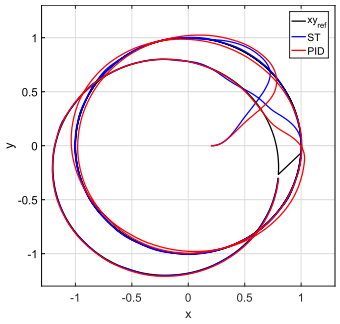

FIGURE 7. SSMR trajectories in the x-y plane, comparison between Super-Twisting and Proportional Integral Derivative.

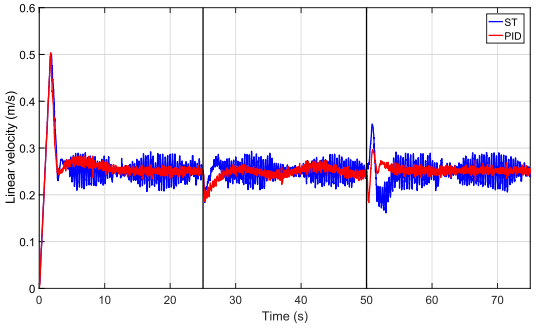

FIGURE 8. Linear velocity reference v_r, comparison between Super-Twisting and Proportional Integral Derivative.

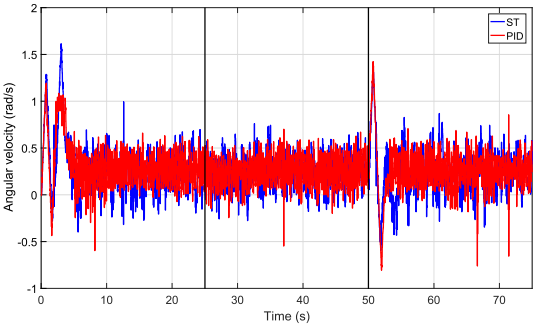

FIGURE 9. Angular velocity reference ω_r, comparison between Super-Twisting and Proportional Integral Derivative.

rate as the ST. During the second cycle, the steady state performance of the HOST far outranks that of the ST. The physical performance is shown in the position plots Fig.12 and Fig.13. The trajectory obtained by the HOST is smoother than the ST. The control inputs are presented in Fig.15 and Fig.16. The chattering for linear velocity is significantly reduced in steady state compared to the ST algorithm. The angular velocity has kept almost the same behavior comparing to ST and PID controllers. The proposed control design using HOST stabilizes double chain of integrators, $\ddot{s}_1$ and $\ddot{s}_2$, by the controllers v_1 and v_2 developed based on Eq.(25). Theses controllers force the sliding variables to zero in finite-time. It can be seen that the controllers act at time 25s and 50s, in order to compensate the perturbation and the parametric uncertainty. Moreover, the chattering is attenuated in all cases comparing to the ST algorithm.

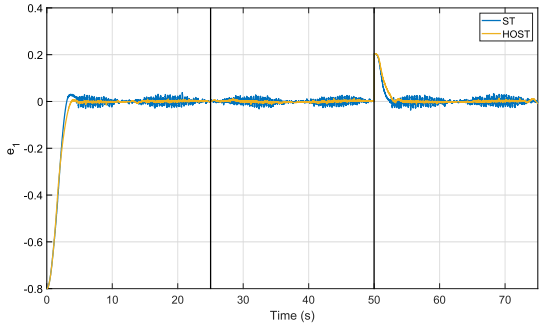

FIGURE 10. Error response e_1, comparison between Higher-Order Super-Twisting and Super-Twisting.

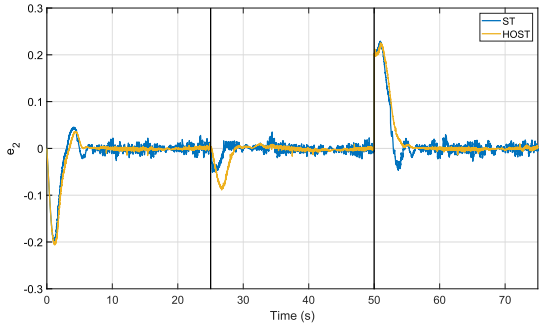

FIGURE 11. Error response e_2, comparison between Higher-Order Super-Twisting and Super-Twisting.

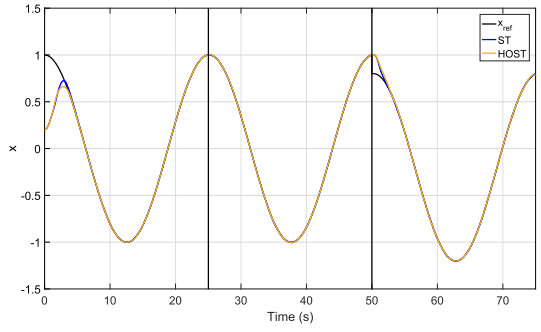

FIGURE 12. Position x response, comparison between Higher-Order Super-Twisting and Super-Twisting.

3) IMAGE PROCESSING VALIDATION

In order to obtain a more significant physical analysis of the robot's performance, image processing was employed during the experiments. "Go Pro Hero 5 Black camera" n 2.7k resolution and 30 frames per second with linear field of view were used at 3 meters elevation above ground and area coverage of 5 $\times$ 2.8 m^2. The robot's movement is tracked using an LED mounted on top, while the experimental area is darkened to improve the image processing speed. The

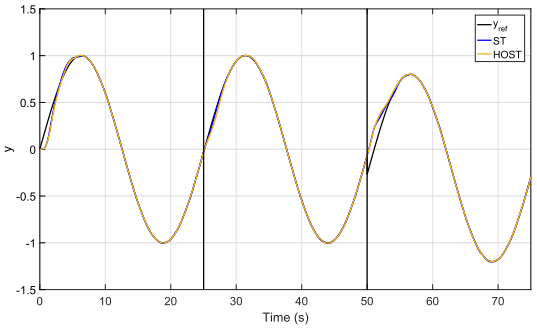

FIGURE 13. Position y response, comparison between Higher-Order Super-Twisting and Super-Twisting.

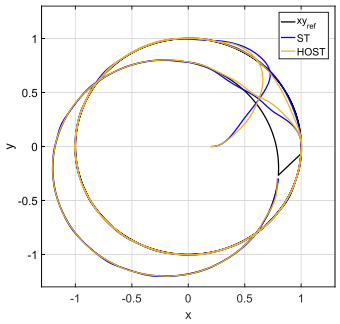

FIGURE 14. SSMR trajectories in the x-y plane, comparison between Higher-Order Super-Twisting and Super-Twisting.

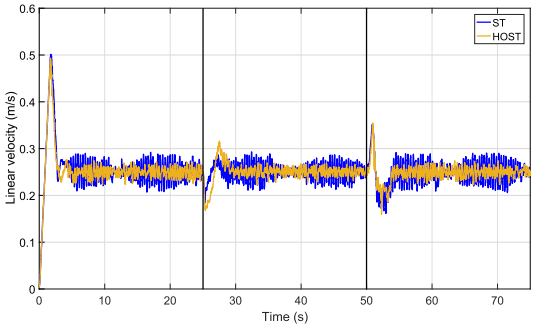

FIGURE 15. Linear velocity reference v_r, comparison between Higher-Order Super-Twisting and Super-Twisting.

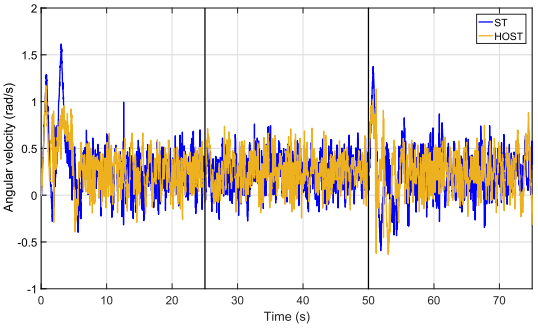

FIGURE 16. Angular velocity reference ω_r, comparison between Higher-Order Super-Twisting and Super-Twisting.

images were processed using Video to Action Shot Sequence (VASS) [33] implemented in Matlab Vision System Toolbox. The algorithm is shown in Fig.17.

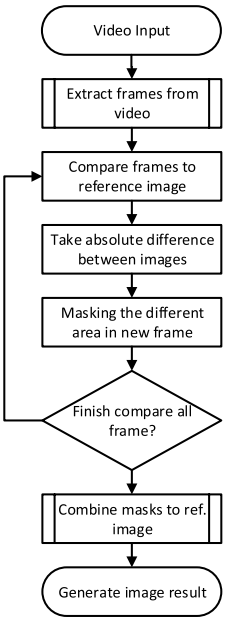

FIGURE 17. Flowchart of the image processing.

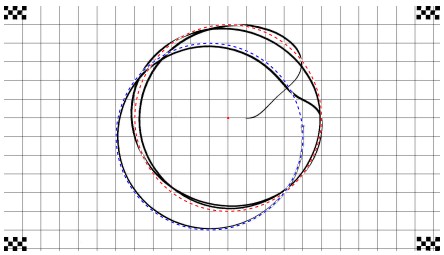

FIGURE 18. Image processing of SSMR trajectories in the x-y plane using PID controller.

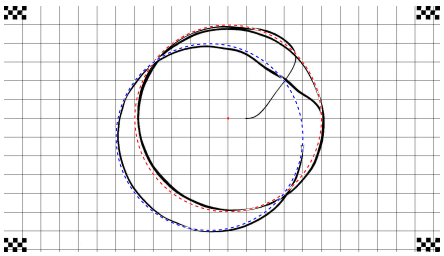

FIGURE 19. Image processing of SSMR trajectories in the x-y plane using Super Twisting controller.

The captured videos used for image processing of the three controller algorithms, PID, ST and HOST, can be seen in the supplemental material of the paper, PID.mp4, ST.mp4 and HOST.mp4, respectively. Fig.18, Fig.19 and Fig.20 show the processed results of the robot performance using the PID, ST and HOST controller respectively. The grid is included to the figure in order to measure the real trajectory of the robot, and two circles red and blue are included to compare with the requested trajectory reference. The red circle is the trajectory during period 1 and 2, and the blue circle is the trajectory

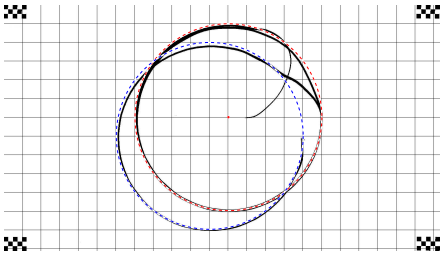

FIGURE 20. Image processing of SSMR trajectories in the x-y plane using Higher-Order Super Twisting controller.

during period 3. The distance between the grids is 20cm. It can be seen that the performances of the controllers have the same behavior with the results discussed in the previous section.

VI. CONCLUSION

A robust trajectory tracking controller for skid steered mobile robot is developed and implemented in this paper. The main objective of the controller is to enable the SSMR to follow a desired trajectory with respect to time through the linear and angular velocities. The control objective is achieved using a Higher-Order Sliding Mode based on Higher-Order Super-Twisting algorithm. The controller has same features of ST such as robustness against uncertainty and external disturbances. In addition, HOST has finite time convergence for higher-order control design and contribute in chattering reduction. The proposed controller is implemented on an SSMR Pioneer 3ATR platform for experimental validation. The experimental results prove the effectiveness of the proposed control design.

APPENDIX A

$$\begin{aligned}
\phi_1 &= \left(\frac{c_{03}+\delta c_3}{c_{01}+\delta c_1}\omega^2 - \frac{c_{04}+\delta c_4}{c_{01}+\delta c_1}v + \right)\cos\theta \\
&\quad - v\omega\sin\theta - d\left(-\frac{c_{05}+\delta c_5}{c_{02}+\delta c_2}v\omega - \frac{c_{06}+\delta c_6}{c_{02}+\delta c_2}\omega \right. \\
&\quad \left. + \frac{\omega_r}{c_{02}+\delta c_2}\right)\sin\theta - d\omega^2\cos\theta - \ddot{x}_r, \\
\gamma_1 &= \frac{v_r}{c_{01}+\delta c_1}\cos\theta, \qquad (33) \\
\phi_2 &= \left(\frac{c_{03}+\delta c_3}{c_{01}+\delta c_1}\omega^2 - \frac{c_{04}+\delta c_4}{c_{01}+\delta c_1}v + \frac{v_r}{c_{01}+\delta c_1}\right)\sin\theta \\
&\quad + v\omega\cos\theta - d\omega^2\sin\theta - \ddot{y}_r \\
&\quad + d\left(-\frac{c_{05}+\delta c_5}{c_{02}+\delta c_2}v\omega - \frac{c_{06}+\delta c_6}{c_{02}+\delta c_2}\omega\right)\cos\theta, \\
\gamma_2 &= \frac{\omega_r}{c_{02}+\delta c_2}\cos\theta. \qquad (34)
\end{aligned}$$

REFERENCES

[1] C. Ordonez, N. Gupta, B. Reese, N. Seegmiller, A. Kelly, and E. G. Collins, "Learning of skid-steered kinematic and dynamic models for motion planning," *Robot. Auto. Syst.*, vol. 95, pp. 207–221, Sep. 2017.
[2] B. Olofsson and L. Nielsen, "Path-tracking velocity control for robot manipulators with actuator constraints," *Mechatronics*, vol. 45, pp. 82–99, Aug. 2017.
[3] L. Caracciolo, A. de Luca, and S. Iannitti, "Trajectory tracking control of a four-wheel differentially driven mobile robot," in *Proc. IEEE Int. Conf. Robot. Autom.*, vol. 4, May 1999, pp. 2632–2638.
[4] W. Yu, O. Y. Chuy, E. G. Collins, and P. Hollis, "Analysis and experimental verification for dynamic modeling of a skid-steered wheeled vehicle," *IEEE Trans. Robot.*, vol. 26, no. 2, pp. 340–353, Apr. 2010.
[5] M. E. Serrano, G. J. E. Scaglia, S. Romoli, V. Mut, and S. Godoy, "Trajectory tracking controller based on numerical approximation under control actions constraints," in *Proc. IEEE Biennial Congr. Argentina (ARGENCON)*, Jun. 2014, pp. 37–42.
[6] M. E. Serrano, G. J. E. Scaglia, F. A. Cheein, V. Mut, and O. A. Ortiz, "Trajectory-tracking controller design with constraints in the control signals: A case study in mobile robots," *Robotica*, vol. 33, no. 10, pp. 2186–2203, Dec. 2015.
[7] F. N. Martins, W. C. Celeste, R. Carelli, M. Sarcinelli-Filho, and T. F. Bastos-Filho, "An adaptive dynamic controller for autonomous mobile robot trajectory tracking," *Control Eng. Pract.*, vol. 16, no. 11, pp. 1354–1363, Nov. 2008.
[8] M. Begnini, D. W. Bertol, and N. A. Martins, "A robust adaptive fuzzy variable structure tracking control for the wheeled mobile robot: Simulation and experimental results," *Control Eng. Pract.*, vol. 64, pp. 27–43, Jul. 2017.
[9] C. Z. Resende, R. Carelli, and M. Sarcinelli-Filho, "A nonlinear trajectory tracking controller for mobile robots with velocity limitation via fuzzy gains," *Control Eng. Pract.*, vol. 21, no. 10, pp. 1302–1309, Oct. 2013.
[10] J. Chen, J. Yu, K. Zhang, and Y. Ma, "Control of regenerative braking systems for four-wheel-independently-actuated electric vehicles," *Mechatronics*, vol. 50, pp. 394–401, Apr. 2018.
[11] M. Boukens, A. Boukabou, and M. Chadli, "Robust adaptive neural network-based trajectory tracking control approach for nonholonomic electrically driven mobile robots," *Robot. Auto. Syst.*, vol. 92, pp. 30–40, Jun. 2017.
[12] E. Maalouf, M. Saad, and H. Saliah, "A higher level path tracking controller for a four-wheel differentially steered mobile robot," *Robot. Auto. Syst.*, vol. 54, no. 1, pp. 23–33, Jan. 2006.
[13] J. Keighobadi, M. S. Sadeghi, and K. A. Fazeli, "Dynamic sliding mode controller for trajectory tracking of nonholonomic mobile robots," *IFAC Proc. Volumes*, vol. 44, no. 1, pp. 962–967, Jan. 2011.
[14] H. Chen, D. Yan, H. Chen, and F. Yang, "A sliding-mode-like design for model-free tracking of nonholonomic mobile robots," in *Proc. 14th Int. Workshop Variable Struct. Syst. (VSS)*, Jun. 2016, pp. 43–46.
[15] H. M. Becerra, J. A. Colunga, and J. G. Romero, "Robust trajectory tracking controllers for pose-regulation of wheeled mobile robots," in *Proc. IEEE/RSJ Int. Conf. Intell. Robots Syst. (IROS)*, Oct. 2016, pp. 1041–1047.
[16] E. S. E. Youssef, N. A. Martins, E. R. De Pieri, and U. F. Moreno, "PD-super-twisting second order sliding mode tracking control for a nonholonomic wheeled mobile robot," *IFAC Proc. Volumes*, vol. 47, no. 3, pp. 3827–3832, 2014.
[17] I. Salgado, D. Cruz-Ortiz, O. Camacho, and I. Chairez, "Output feedback control of a skid-steered mobile robot based on the super-twisting algorithm," *Control Eng. Pract.*, vol. 58, pp. 193–203, Jan. 2017.
[18] A. Salome, A. Y. Alanis, and E. N. Sanchez, "Discrete-time sliding mode controllers for nonholonomic mobile robots trajectory tracking problem," in *Proc. 8th Int. Conf. Electr. Eng., Comput. Sci. Autom. Control*, Oct. 2011, pp. 1–6.
[19] I. Gonzalez-Hernandez, S. Salazar, F. Munoz, and R. Lozano, "Super-twisting control scheme for a miniature quadrotor aircraft: Application to trajectory-tracking problem," in *Proc. Int. Conf. Unmanned Aircr. Syst. (ICUAS)*, Jun. 2017, pp. 1547–1554.
[20] A. Rezoug, M. Hamerlain, Z. Achour, and M. Tadjine, "Applied of an adaptive higher order sliding mode controller to quadrotor trajectory tracking," in *Proc. IEEE Int. Conf. Control Syst., Comput. Eng. (ICCSCE)*, Nov. 2015, pp. 353–358.
[21] A. Levant, "Finite-time stability and high relative degrees in sliding-mode control," in *Sliding Modes After the First Decade of the 21st Century*, L. Fridman, J. Moreno, and R. Iriarte, Eds. Berlin, Germany: Springer, 2012, pp. 59–92.

[22] A. Chalanga, S. Kamal, L. M. Fridman, B. Bandyopadhyay, and J. A. Moreno, "Implementation of super-twisting control: Super-twisting and higher order sliding-mode observer-based approaches," *IEEE Trans. Ind. Electron.*, vol. 63, no. 6, pp. 3677–3685, Jun. 2016.
[23] C. Edwards and Y. B. Shtessel, "Adaptive continuous higher order sliding mode control," *Automatica*, vol. 65, pp. 183–190, Mar. 2016.
[24] I. Castillo, F. Castanos, and L. Fridman, "Sliding surface design for higher-order sliding modes," in *Recent Trends in Sliding Mode Control*. London, U.K.: Institute of Engineering and Technology (IET), 2016, pp. 29–56.
[25] I. Matraji, A. Al-Durra, A. Haryono, K. Al-Wahedi, and M. Abou-Khousa, "Trajectory tracking control of skid-steered mobile robot based on adaptive second order sliding mode control," *Control Eng. Pract.*, vol. 72, pp. 167–176, Mar. 2018.
[26] S. Laghrouche, M. Harmouche, and Y. Chitour, "Higher order super-twisting for perturbed chains of integrators," *IEEE Trans. Autom. Control*, vol. 62, no. 7, pp. 3588–3593, Jul. 2017.
[27] S. Laghrouche, F. Plestan, and A. Glumineau, "Higher order sliding mode control based on integral sliding mode," *Automatica*, vol. 43, no. 3, pp. 531–537, Mar. 2007.
[28] L. Fridman and A. Levant, "Higher-order sliding modes," *Sliding Mode Control Eng.*, vol. 11, pp. 53–102, Jan. 2002.
[29] A. Levant, "Sliding order and sliding accuracy in sliding mode control," *Int. J. Control*, vol. 58, no. 6, pp. 1247–1263, Dec. 1993.
[30] Y. Hong, "Finite-time stabilization and stabilizability of a class of controllable systems," *Syst. Control Lett.*, vol. 46, no. 4, pp. 231–236, Jul. 2002.
[31] Y. Hong, G. Yang, D. Cheng, and S. Spurgeon, "Finite time convergent control using terminal sliding mode," *J. Control Theory Appl.*, vol. 2, no. 1, pp. 69–74, Feb. 2004.
[32] A. Levant and L. Fridman, "Robustness issues of 2-sliding mode control," in *Variable Structure Systems: From Principles to Implementation*. WordPress, 2004, pp. 129–154.
[33] A. Knaack, M. Karp, and E. Shin. (2015). *Video to Action Shot Sequence*. [Online]. Available: https:/actionsequence.wordpress.com/

IMAD MATRAJI (Member, IEEE) received the master's degree in engineering and management of industrial systems and the Ph.D. degree in automatic control system from the University of Technology of Belfort-Montbeliard (UTBM), France, in 2009 and 2013, respectively. In 2014, he joined Hydrogen South Africa with the University of Western Cape, South Africa, as a Postdoctoral Researcher. In 2015, he joined Khalifa University, Abu Dhabi, United Arab Emirates, as a Research Associate. In 2017, he joined Great Wall Motor as the Chief Engineer Fuel Cell Control System. His research interests include PEM fuel cell control systems for automotive application, renewable energy management and power systems, and robotics.

KHALED AL-WAHEDI (Member, IEEE) received the B.Sc. and M.Sc. degrees from Case Western Reserve University, in 1999 and 2000, respectively, and the Ph.D. degree from Imperial College London, in 2009, all in electrical engineering. He is currently an Assistant Professor with Khalifa University, United Arab Emirates. His current research interests include computational complexity, optimization, and robotics.

AHMED AL-DURRA (Senior Member, IEEE) received the Ph.D. degree in ECE from The Ohio State University in 2010. He is currently an Associate Professor with the ECE Department, Khalifa University, United Arab Emirates. His research interests are applications of control and estimation theory on power systems stability, micro and smart grids, renewable energy systems and integration, and process control. He has one U.S. patent, one edited book, 12 book chapters, and more than 200 scientific articles in top-tier journals and refereed international conference proceedings. He has supervised/co-supervised more than 25 Ph.D./master's students. He is also leading the Energy Systems Control and Optimization Lab under the Advanced Power and Energy Center, an Editor of the IEEE TRANSACTIONS ON SUSTAINABLE ENERGY and the IEEE POWER ENGINEERING LETTERS, and an Associate Editor of the IEEE TRANSACTIONS ON INDUSTRY APPLICATIONS and *Frontiers in Energy Research*–Smart Grids.